Mode II Fracture Behavior of Parallel Strand Bamboo Measured by 3-Point End-Notched Flexure Tests

Zhen-wen Zhang,[a] Jia-liang Zhang,[b] Yu-shun Li,[d,*] and Rui Liu [c]

Parallel strand bamboo (PSB) is a new type of bio-composite. In the present study, three-point bend end-notched flexure (3ENF) tests of PSB were conducted to analyze the fracture behavior including fracture process, resistant curves, and critical energy release rate in the longitudinal (L) system. The results show that transverse-longitudinal (TL) and thickness-longitudinal (ZL) specimens had the same fracture process including the stages of fracture process zone (FPZ) development and opening crack propagation but different mode II critical energy release rate (G_{IIc}), and they indicate that the fiber bridging had a significant influence. The fracture processes suggest the PSB specimens of which the initial crack length was 0.5 times the half span had a stable crack propagating process, and the crack propagation length was wide enough to evaluate G_{IIc}, which was 5.02 N·mm^{-1} of TL specimens and 2.71 N·mm^{-1} of ZL specimens. Besides, there was no obvious influence of span/depth ratio on the fracture resistance of both ZL and TL specimens when the ratio was larger than 15.

Keywords: Parallel strand bamboo; Mode II fracture; Critical energy release rate; Fracture resistant curve

Contact information: a: School of Civil and Environmental Engineering, Ningbo University, Ningbo, P.R. China, 315211; b: College of Science & Technology, Ningbo University, Ningbo, P.R. China, 315300; c: College of Architecture and Environmental Design, Kent State University, Kent, OH, USA, 44242; d: Construction Engineering College, Qingdao Agricultural University, Qingdao, P.R. China, 266109;
** Corresponding author: lys0451@163.com*

INTRODUCTION

Parallel strand bamboo (PSB) is a new type of bio-composite that can be used as an excellent sustainable construction material because of its outstanding attributes (Li *et al.* 2015, 2017; Zhang *et al.* 2019). To effectively use PSB as a structural material, a better understanding of its mechanical properties, including the fracturing properties, is required.

PSB is usually fabricated by gluing of bamboo strands through high pressure and then forming the material into boards. The bamboo strands are layered and aligned with each other in the parallel-to-grain direction, and therefore the bamboo fibers of PSB distribute in the same direction. As a result, PSB can be treated as a wood-like material and be considered as an orthotropic material, with a local symmetry material coordinate (Fig. 1). The longitudinal axis (L) is parallel to the direction of fibers; the transverse axis (T) is perpendicular to the fibers; and the thickness axis is (Z). The crack propagation in the L system was investigated in the present study. It is one of the most frequent crack propagation systems in timber beams as well as PSB beams (Smith and Vasic 2003; Huang *et al*. 2015). Therefore, a fundamental requirement is to measure mode I and mode II fracture properties.

To obtain the fracture properties of solid wood, the double cantilever beam (DCB) and three-point bend end-notched flexure (3ENF) tests have been used in recent years as the principal methods (De Moura *et al*. 2009; Yoshihara and Satoh 2009; Xavier *et al*. 2015). Moreover, Yoshihara (2010) adopted these methods to wood-like materials. Therefore, these methods are expected to be extended to measure the fracture properties of PSB, and several studies have reported the investigation of the fracturing properties of PSB (Huang *et al*. 2018a; Wang *et al*. 2019).

In this study, 3ENF tests of PSB were conducted, and the fracture behaviors including fracture process, resistant curves (R-curves,) and critical energy release rate were analyzed. Fracture properties of both TL and ZL system were examined, and the compliance-based beam method (De Moura *et al*. 2009) was employed to obtain R-curves.

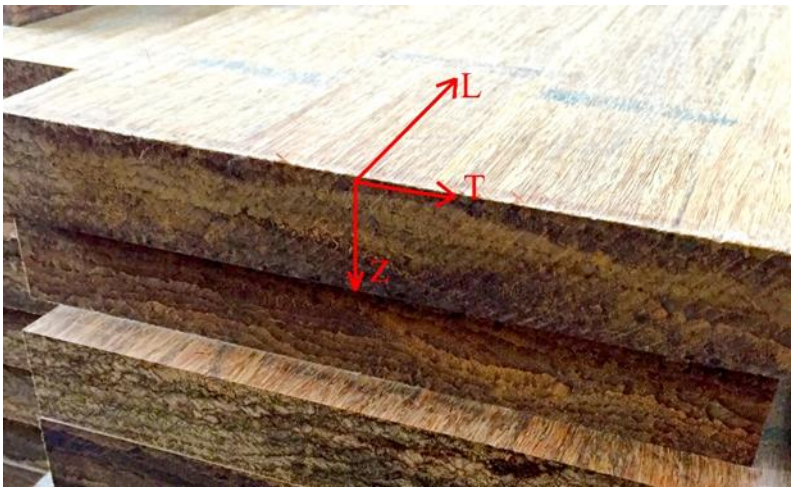

Fig. 1. PSB boards and the coordinate system (L, T, and Z represent the longitudinal axis parallel to the direction of fibers, the transverse axis perpendicular to the fibers and the thickness axis respectively)

EXPERIMENTAL

Materials

A PSB board was used to get the specimens for testing and was fabricated by Phyllostachys, a common bamboo genus in China. All specimens were cut from this same PSB board. According to the PSB fabricating process, it is natural to define the parallel-to-grain, perpendicular-to-grain and thickness directions of the PSB boards as the L-axis, T-axis, and Z-axis, respectively (Fig. 1), and the elastic properties of PSB in this coordinate system are given in Table 1.

3ENF Tests

Figure 2 shows the configuration of 3ENF specimens and the diagram of the tests. Table 2 lists the dimensions tested in this study. There were 6 groups with 5 specimens each according to the span-to-depth ratio ($2L/2h$) and the initial crack length, which are two constraint parameters of the specimen dimensions.

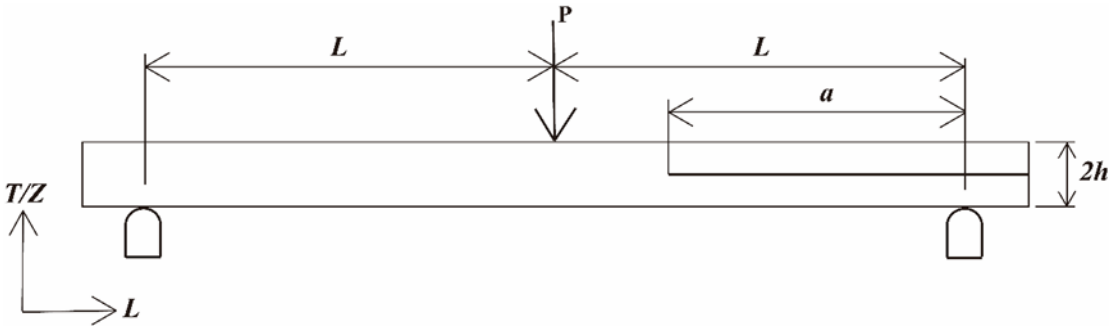

(a) Specimen configuration (*a* presents initial crack length)

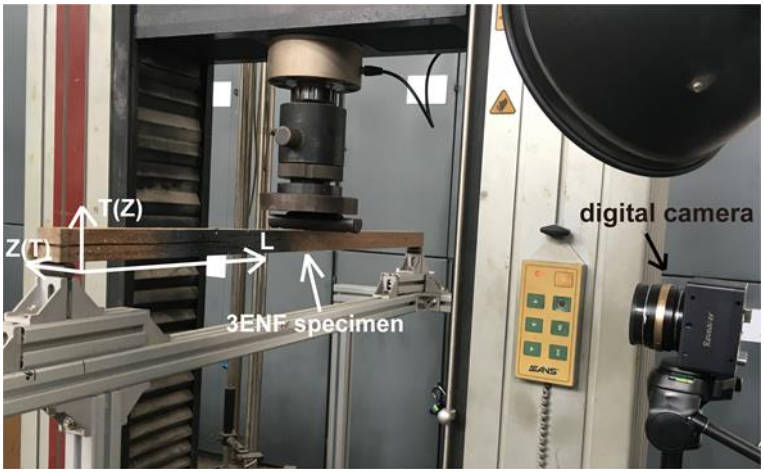

(b) Test setup

Fig. 2. Specimen configuration and test setup

Table 1. Elastic Properties of PSB

E_L (MPa)	E_T (MPa)	E_Z (MPa)	G_{TL} (MPa)	G_{ZL} (MPa)	μ_{TL}	μ_{ZL}
14171	2065	1810	2829	2744	0.31	0.30

Table 2. Specimen Dimension

Span (2*L*) (mm)	Depth (2*h*) (mm)	Width (*b*) (mm)	Crack Length (*a*) (mm)	2*L*/2*h*	*a*/*L*
450	30	30	113	15	0.5
750	30	30	188	25	0.5
900	30	30	225	30	0.5

To measure the mode II fracture toughness of wood by ENF tests, the influence of additional deflection caused by shear should be taken into account (Yoshihara 2001). As listed in Table.1, the elastic properties of PSB are similar to wood, and therefore the shear deformation in bending tests has to be considered as well and control $2L/2h > 15$ to reduce this influence.

According to linear fracture mechanics, a fracture propagates unstably in the 3ENF tests of linear elastic materials if the initial crack length is smaller than 0.7 times the half span ($a_0 < 0.7L$). However, Yoshihara (2001) also found the crack propagated stably under the condition of $a_0 = 0.5$L. Considering $a_0 < 0.7$L has been checked in the previous study

(Wang *et al.* 2019), the specimens with the initial crack length of 0.5 *L* was tested in this study to investigate the crack propagate process of PSB.

The initial crack was first machined by a band saw with1 mm thickness, and then it was extended to 1 to 2 mm at the tip by a cutting blade. The alignment of the crack front was verified by measuring the extended crack length on both sides. After the crack was cut, one piece of Teflon film with 0.13 mm thickness was inserted between the initial crack surfaces to minimize the influence of friction when crack propagating. A speckle pattern was spray-painted on the specimens to obtain the strain field around the crack tip and the crack propagating process using the digital image correlation (DIC) method.

Compliance-based Beam Method

The method is based on specimen compliance and on the equivalent crack concept (De Moura *et al.* 2009). The specimen compliance at the loading point during crack propagation as shown in Fig. 1 can be obtained from,

$$C = \frac{3a_{eq}^3+2L^3}{8E_f Bh^3} + \frac{3L}{10GBh} \quad (1)$$

where *G* is the shear modulus, a_{eq} is the equivalent crack length and E_f is the estimate of flexural modulus considering the initial crack length (a_0) and the initial compliance (C_0). a_{eq} and E_f can be obtained from Eqs. 2 and 3, respectively,

$$a_{eq} = \left[\frac{C_{corr}}{C_{0corr}} a_0^3 + \frac{2}{3}\left(\frac{C_{corr}}{C_{0corr}} - 1\right) L^3\right]^{\frac{1}{3}} \quad (2)$$

$$E_f = \frac{3a_0^3+2L^3}{8Bh^3 C_{0corr}} \quad (3)$$

where C_{0corr} is given by Eq. 4.

$$C_{0corr} = C_0 - \frac{3L}{10GBh} \quad (4)$$

C_{corr} is obtained from Eq. (4) with the current compliance *C* instead of C_0. Combining the Irwin-Kies equation (Kanninen and Popelar 1985) with Eq. (1), the energy release rate can be expressed as follows, where *P* is applied load.

$$G_{II} = \frac{9P^2 a_{eq}^2}{16B^2 E_f h^3} \quad (5)$$

RESULTS AND DISCUSSION

Load-Displacement Relationships

Figure 3 illustrates the typical load-displacement curves of different spans and coordinate systems and indicates that the fracture behavior was similar despite spans and coordinate systems. The decline of the curves suggests that there was a stable fracture growth process of all the specimens. This becomes even clearer when considering the resistance curves (R-curves) shown in the following section. The curves also indicate that the specimens of ZL system have smaller fracture toughness than the specimens of TL systems because of the different maximum load between TL and ZL systems of the same span.

The fracture process was also examined by the DIC method. Figure 4 shows the strain variation images near the crack tip of the different stages in fracture process obtained

by DIC. The development of the fracture process zone (FPZ) and the crack propagation process can be observed in the image sequence. The sequence from Fig. 4(a) to 4(c) shows the extension of stress concentration near the crack tip, which is known as FPZ. Crack propagation is observed in Figs. 4(c) to 4(f), and FPZ was relatively stable.

The fracture process obtained by load-displacement relationships and DIC results suggests a stable crack propagation of the specimens. This phenomenon is different from the conclusion of linear fracture mechanics, which considers unstable fracture propagation when the initial crack length is smaller than 0.7 times the half span ($a_0 < 0.7L$). The reason may be the nonlinear behavior of PSB caused by the fiber bridging between fracture surfaces (Huang *et al*. 2015), which is not considered in the linear fracture mechanics.

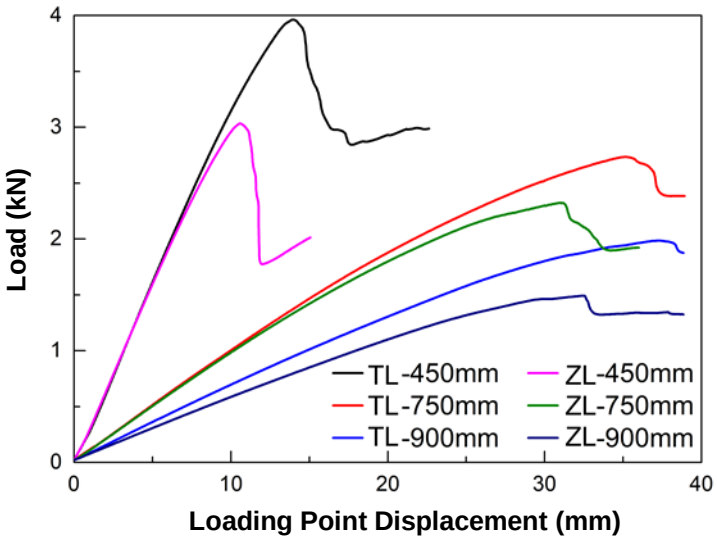

Fig. 3. Typical load-displacement curves of TL and ZL systems

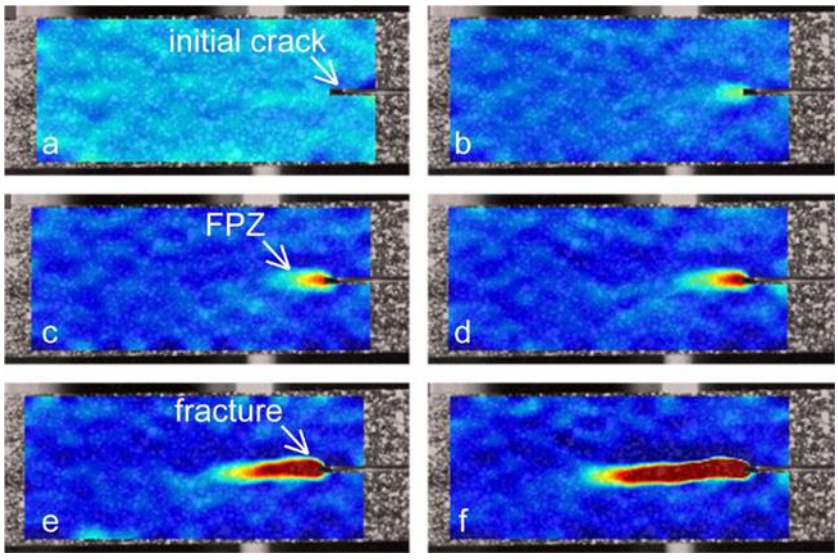

Fig. 4. Strain contour of fracture process obtained by DIC (a. initial crack; b & c. FPZ developing process; d, e & f: fracture developing process; the color changes from blue to red as stress increases, and the dark red area means an opened crack exists)

Fracture-resistant Curves

Figure 5 shows the typical mode II fracture-resistant curves (R-curves) of specimens with a 900 mm span in TL and ZL system. The horizontal axis represents the increase of crack propagation length, while the vertical axis "G_{II}" represents the corresponding mode II energy release rate, and the original means the initiation of crack propagation.

Figure 5 shows that G_{II} increased after the crack propagation initiation. This stage is regarded as the process of FPZ development, and this increase is the result of fiber bridging phenomenon between the crack surfaces, which are commonly observed in the crack propagation of solid wood and wood products (Yoshihara 2010; Huang *et al*. 2018b).

Considering the FPZ development revealed by DIC and R-curves in Fig. 5, it was concluded that the fracture resistances increased with FPZ development until the initiation of the opening crack extension and a critical energy release rate (G_{IIc}) was achieved, and this also means the FPZ length had reached its maximum length. The value of G_{IIc} was several times of initial value, which suggests that the influence of the fiber bridging was significant relative to mode II fracture resistance by 3ENF tests.

At the end of the opening crack extension, the crack tip approached the midspan, and the value of G_{II} obviously increased because of the influence of the compression stresses near the loading point.

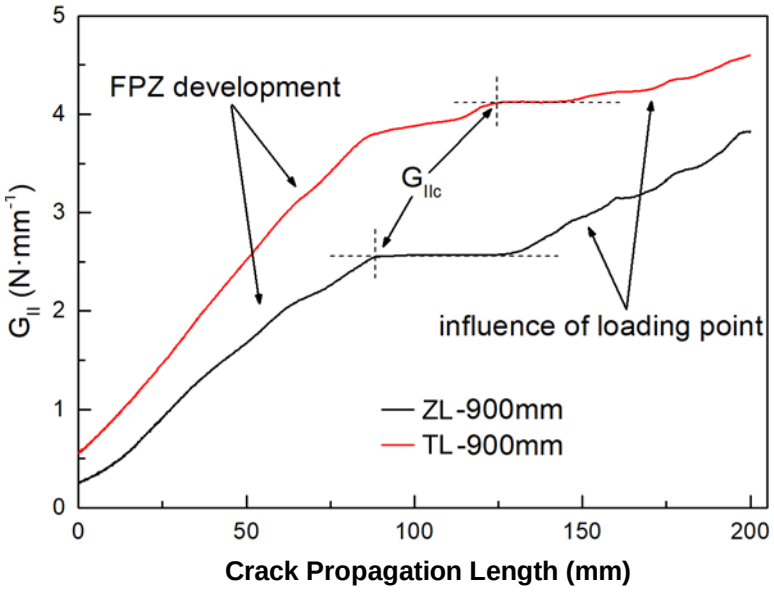

Fig. 5. Typical R-curves of TL and ZL system (The crack propagation length is the difference between the initial crack length and equivalent crack length calculated by Eq. 2)

Critical Energy Release Rate

Figure 6 shows the mean values of G_{IIc} obtained from the tests. The TL specimens had a stronger fracture resistance than ZL specimens. This characteristic could be explained by the fabricating procedure of PSB. Although the mode II fracture behavior of PSB is controlled by delamination, it is influenced by the fiber bridging to some extent between the TL- and ZL-system. The bamboo strands are arranged layer by layer in one direction. This causes a better laminated structure in the TL-system than in the ZL-system. Therefore, the crack propagates mainly along the adhesive layer between bamboo strands in the ZL-

system, while the crack goes relatively more through the bamboo strands in the TL-system. This leads to more influence of fiber bridging on fracture resistance when crack propagation is evaluated in TL specimens. The randomness of fiber bridging probably is the reason for the higher standard deviation values.

Figure 6 also shows that the influence of span/depth ratio was not significant relative to the value of G_{IIc} of both TL and ZL specimens. The G_{IIc} value could be affected by the additional deflection caused by shear deformation, which was not obvious in this study.

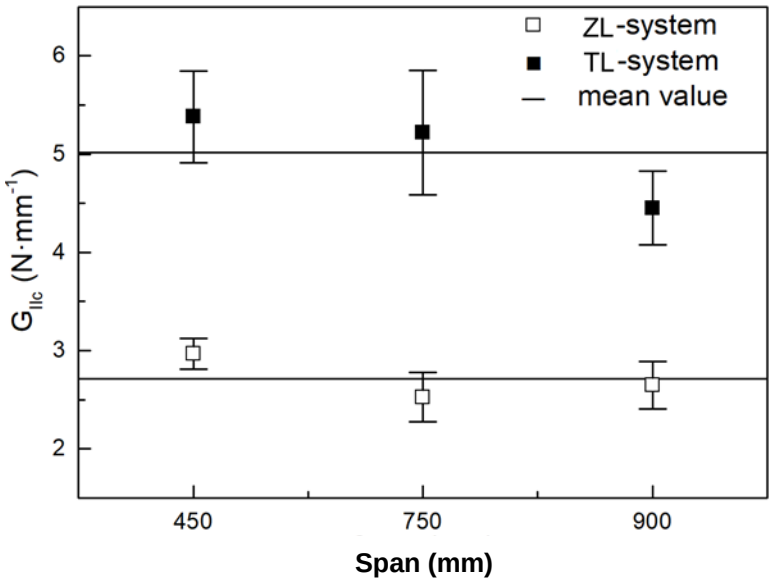

Fig. 6. Critical energy release rate of TL and ZL system

CONCLUSIONS

1. The fracture behavior of transverse-longitudinal (TL) and thickness-longitudinal (ZL) specimens of parallel strand bamboo (PSB) were investigated by three-point bend end-notched flexure (3ENF) tests. The results show that the fracture process of PSB contains the stages of fracture process zone (FPZ) development and opening crack propagation, which is similar to the solid wood.
2. The mode II fracture behavior of PSB is influenced by fiber bridging in addition to delamination because of misalignment in the presence of bamboo strands (bamboo fibers). The bamboo strands are arranged layer by layer in one direction, which means more misalignment of bamboo fibers in the TL-system. This causes more influence of fiber bridging on fracture resistance when crack propagates relatively more through the bamboo strands in the TL-system in TL specimens, as the R-curves and critical energy release rate indicate.
3. The fracture processes analyzed by load-displacement relationships, DIC results, and R-curves indicate that TL and ZL specimens had the same fracture process generally, and show that the PSB specimens of which the initial crack length was 0.5 times the half span (a_0 = 0.5 L) had a stable crack propagating process. Moreover, the range of the crack propagation length was wide enough to evaluate the R-curve behavior of TL

and ZL specimens, and the 3ENF test was appropriate for measuring the critical energy release rate.

4. The critical energy release rate of TL and ZL specimens were also calculated using CBBM. However, the TL and ZL specimens had distinguishable mode II fracture resistances that is 5.02 $N \cdot mm^{-1}$ of TL specimens while it was 2.71 $N \cdot mm^{-1}$ of ZL specimens. Besides, the span/depth ratio examined in this study shows no obvious influence on the fracture resistance of both ZL and TL specimens.

ACKNOWLEDGEMENTS

This work was supported by the National Natural Science Foundation of China (No.51708304, 51978345), National Key Research and Development Program of China (No.2017YFC0703502), and Ningbo Natural Science Foundation (No. 2018A610349). The authors also gratefully acknowledge support from the K.C. Wong Magna Fund and the Liu Kong Aiju Education Fund at Ningbo University.

REFERENCES CITED

De Moura, M. F. S. F., Silva, M. A. L., Morais, J. J. L., De Morais, A. B., and Lousada, J. J. L. (2009). "Data reduction scheme for measuring GIIc of wood in end-notched flexure (ENF) tests," *Holzforschung* 63(1), 99-106. DOI: 10.1515/HF.2009.022

Huang, D., Bian, Y., Zhou, A., and Sheng, B. (2015). "Experimental study on stress–strain relationships and failure mechanisms of parallel strand bamboo made from Phyllostachys," *Construction and Building Materials* 77, 130-138. DOI: 10.1016/j.conbuildmat.2014.12.012. DOI: 10.1016/j.conbuildmat.2014.12.012

Huang, D., Pan, W., Zhou, A., Wang X. and Xu, J. (2018a). "Experimental study on mode II fracture characteristics of parallel strand bamboo," *Journal of Southeast University (Natural Science Edition)* 48(6), 1076-1081. DOI: 10.3969/j.issn.1001-0505.2018.06.013

Huang, D., Sheng, B., Shen, Y. and Chui, Y. (2018b). "An analytical solution for double cantilever beam based on elastic–plastic bilinear cohesive law: Analysis for mode I fracture of fibrous composites," *Engineering Fracture Mechanics* 193, 66-76. DOI: 10.1016/j.engfracmech.2018.02.019

Kanninen, M. F., and Popelar, C. H. (1985). *Advanced Fracture Mechanics*, Oxford University Press, UK.

Li, Y., Shan, W., Shen, H., Zhang, Z. W., and Liu, J. (2015). "Bending resistance of I-section bamboo-steel composite beams utilizing adhesive bonding," *Thin-Walled Structures* 89,17-24. DOI: 10.1016/j.tws.2014.12.007

Li, Y., Yao, J., Li, R., Zhang, Z., and Zhang, J. (2017). "Thermal and energy performance of a steel-bamboo composite wall structure," *Energy and Buildings* 156, 225-237. DOI: 10.1016/j.enbuild.2017.09.083

Smith, I. and Vasic, S. (2003). "Fracture behaviour of softwood," *Mechanics of Materials* 35(8), 803-815. DOI: 10.1016/S0167-6636(02)00208-9

Xavier, J., Fernandes, J. R. A., Morais, J. J. L., and Frazão, O. (2015). "Fracture behaviour of wood bonded joints under modes i and II by digital image correlation

and fibre Bragg grating sensors," *Ciencia e Tecnologia dos Materiais* 27(1), 27-35. DOI: 10.1016/j.ctmat.2015.06.001

Yoshihara, H. (2001). "Influence of span/depth ratio on the measurement of mode II fracture toughness of wood by end-notched flexure test," *Journal of Wood Science* 47, 8-12. DOI: 10.1007/BF00776638

Yoshihara, H. (2010). "Mode I and mode II initiation fracture toughness and resistance curve of medium density fiberboard measured by double cantilever beam and three-point bend end-notched flexure tests," *Engineering Fracture Mechanics* 77, 2537-2549. DOI: 10.1016/j.engfracmech.2010.06.015

Yoshihara H., and Satoh, A. (2009). "Shear and crack tip deformation correction for the double cantilever beam and three-point end-notched flexure specimens for mode I and mode II fracture toughness measurement of wood," *Engineering Fracture Mechanics* 76, 335-346. DOI: 10.1016/j.engfracmech.2008.10.012

Wang, X., Zhou, A., and Chui Y. (2019). "Experimental investigation of mode II fracture properties of parallel strand bamboo composite by end notched flexure test," *BioResources* 14(1), 1579-1590. DOI: 10.15376/biores.14.1.1579-1590

Zhang, Z. W., Li, Y. S., Liu, R., and Zhang, J. L. (2019). "Low energy impact on the interface of bamboo-steel composites," *The Journal of Adhesion* 95(12), 1057-1074. DOI: 10.1080/00218464.2018.1466705

Article submitted: January 2, 2020; Peer review completed: March 14, 2020; Revised version received and accepted: March 17, 2020; Published: March 20, 2020.
DOI: 10.15376/biores.15.2.3219-3227